Contactless analysis of surface passivation and charge transfer at TiO_2–Si interface

Ramsha Khan[a†], Xiaolong Liu[b†], Ville Vähänissi[b], Harri Ali-Löytty[c], Hannu P. Pasanen[a], Hele Savin[b*], Nikolai V. Tkachenko[a*]

a. Photonic Compounds and Nanomaterials Group, Faculty of Engineering and Natural Sciences, Tampere University, P.O. Box 541, FI-33014 Tampere University, Finland

b. Department of Electronics and Nanoengineering, Aalto University, Tietotie 3, 02150 Espoo, Finland

c. Surface Science Group, Faculty of Engineering and Natural Sciences, Tampere University, P.O. Box 692, FI-33014 Tampere University, Finland

† Both of the authors contributed equally to this article.

*E-mail: hele.savin@aalto.fi; nikolai.tkachenko@tuni.fi

1. Optical properties

In order to confirm the thickness of TiO_2 thin films prepared by ALD, cross-sectional SEM images of the TiO_2/Si samples were taken. The image for as-dep TiO_2/n-Si is shown in **Figure S1** which confirms the film thickness to be 50-55 nm. The steady state reflectance of all the as-dep. TiO_2/Si samples is shown in **Figure S2** which shows that the reflectance of Si decreases as TiO_2 thin layers are deposited over it. According to the theory of quarter-wavelength anti-reflection coating ($d = \lambda/4n_{TiO2}$, d is the thickness and n_{TiO2} is the refractive index of TiO_2), the (first-order) wavelength at minimum reflection red-shifts as the film thickness increases. Since the spectra shifts to red region with TiO_2 on Si, the samples have better ability to absorb light. Hence, TiO_2 also acts as an anti-reflective coating.

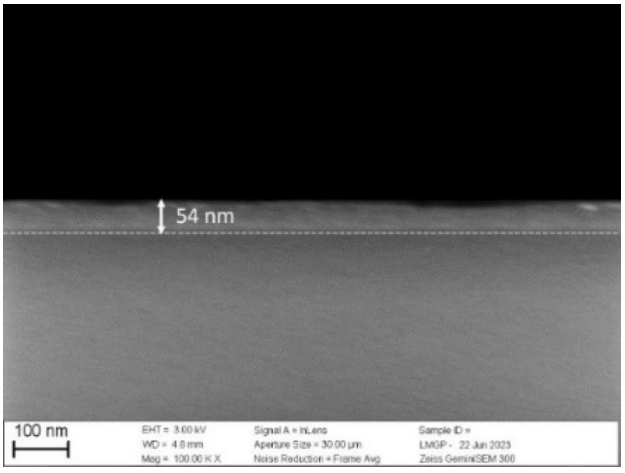

Figure S1: *Cross-section SEM image of as-dep. TiO_2/n-Si sample.*

2. Steady state reflectance spectra

As the samples were prepared to analyze both the passivation and charge transfer within the TiO_2/Si heterojunctions, the thickness of the TiO_2 films was optimized accordingly. For TR spectroscopy measurements, a suitable interference pattern was required to clearly study the charge transfer TR signal from TiO_2. Therefore, this interference pattern was induced by changing the thickness of TiO_2 film which brings changes in the steady-state reflectance spectra of the TiO_2/Si heterojunctions.

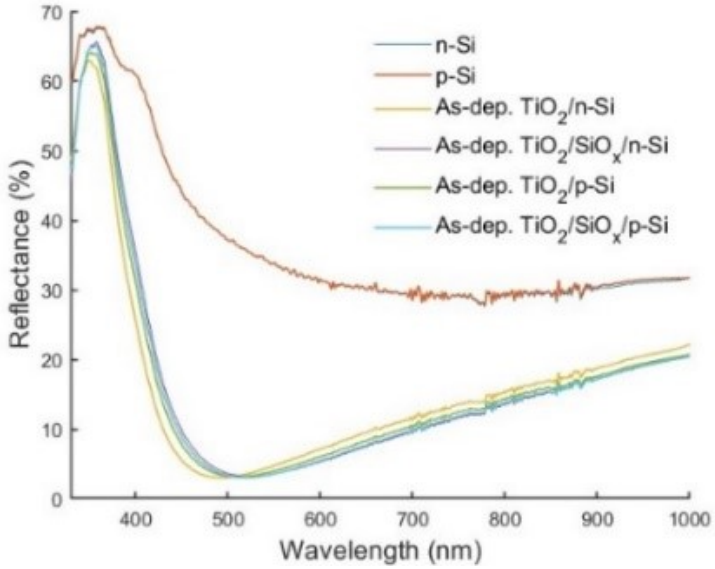

Figure S2: *Steady state reflectance spectra of the bare substrates and TiO_2/Si heterojunctions.*

3. Resistivity range for the n- and p-Si

The nominal resistivity of the Si wafer is 1-5 Ohm cm. However, during lifetime measurement, the resistivity is also measured (each wafer was measured from 4+ spots with 8+ measurements). The resistivity of n-type Si samples is between 2.15-2.20 Ohm cm and of p-type Si samples is between 2.49-2.56 Ohm cm.

			Resistivity (Ohm cm)	
Wafer ID	Type	Comment	Minimum	Maximum
B4304	N	55 nm TiO2/300C anneal	2.17	2.2
B4323	N	55nm TiO2/SiO2	2.15	2.18
B4324	N	55 nm TiO2	2.19	2.2
EH17	P	55 nm TiO2/300C anneal	2.52	2.54
EH10	P	10 nm TiO2/SiO2	2.49	2.52
EH13	P	55 nm TiO2	2.53	2.55
EH14	P	55nm TiO2/SiO2	2.54	2.56

4. Effective carrier lifetime and surface recombination velocity

Table S1: *Effective lifetimes (τ_{eff}) for HF-dipped and RCA2 oxidized Si wafers and TiO_2 deposited Si wafers with their corresponding surface recombination velocities ($S_{eff,max}$) at an injection level of 1E15 cm^{-3}.*

Sample	τ_{eff} *(µs)*	$S_{eff,max}$ *(cm s^{-1})*
As-dep. TiO_2/n-Si	1230	11.4
As-dep. TiO_2/p-Si	689	20.3
As-dep. TiO_2/SiO_x/n-Si	531	26.4
As-dep. TiO_2/SiO_x/p-Si	320	43.8

5. Surface passivation analyzed in different TiO_2/Si heterojunctions

Table S2: *Surface passivation of Si with TiO_2 thin films analyzed by different research groups.*

Si doping type	*Si resistivity (Ω cm)*	*Si thickness (µm)*	*Pre-ALD treatment*	*TiO_2 Precursor*	*ALD temperature (°C)*	*TiO_2 thickness (nm)*	*Annealing temperature (°C)*	*Annealing time (min)*	*Annealing Ambient*	*Teff (µs)*	*Seff (cm/s)*	*Reference*	*Year*
n	**1**	**190**	**Thermal oxidation**	**$TiCl_4$**	**75**	**5.5**	**250**	**3**	**N2+H2**	**850**	**11**	1	**2016**
p	**10**	**240**	**HF**	**TDMAT**	**150**	**1.5**	**350**	**15**	**N2+H2**	**840**	**14**	2	**2016**
p	**5000**	**275**	**HF**	**$TiCl_4$**	**80**	**114**	**As-deposited**	**-**	**-**	**1584**	**8.7**	3	**2018**
n	**2-5**	**280**	**HNO3**	**TDMAT**	**150**	**3**	**400**	**3**	**Ar+H2**	**891**	**16**	4	**2020**
n	**2-5**	**280**	**SC2 (RCA2)**	**TDMAT**	**150**	**3**	**350**	**3**	**Ar+H2**	**1687**	**9.6**	5	**2020**
n	**2-4**	**280**	**SC2 (RCA2)**	**TDMAT**	**175**	**3**	**275**	**3**	**Ar+H2**	**1800**	**-**	6	**2021**
n	**2/2.5**	**280**	**HF**	**$TiCl_4$**	**100**	**60**	**250**	**30**	**N2**	**~1200**	**11.7**	7	**2021**

6. Charge transfer spectra extraction

To study the CT across Si and TiO_2 interface, transient reflectance spectroscopy was utilized. By this technique, one can measure the change in reflectance of the films upon photoexcitation. The samples were excited at 500 nm (with an energy density of 200 µJ cm^{-2}) from the polished side of the samples to selectively generate the photocarriers in Si part of the samples.[8] The CT spectra extraction for as-dep. TiO_2/p-Si, TiO_2/SiO_x/p-Si, and TiO_2/SiO_x/n-Si samples are shown in **Figure S3-Figure S5.**

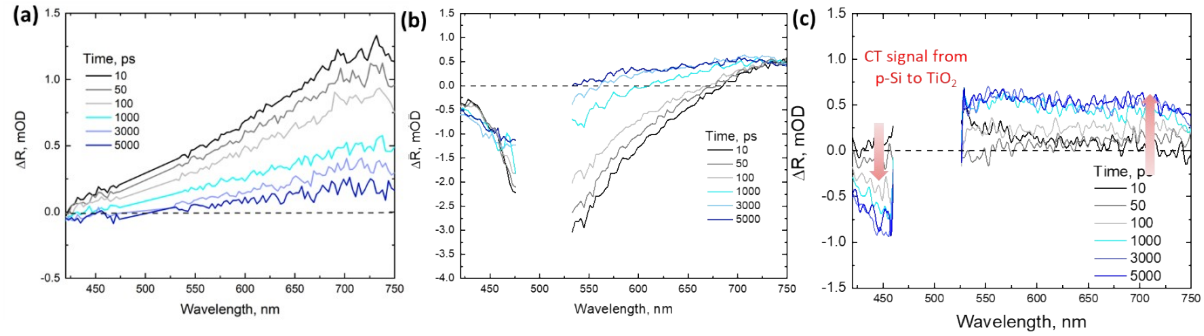

Figure S3: *Excitation of samples at 500 nm to obtain TR spectra of (a) bare HF-treated p-Si substrate at different delay times, (b) as-dep.-TiO_2/p-Si sample at different delay times, and (c) extracted CT spectra of as-dep. TiO_2/p-Si sample. The arrows indicate electrons moving from p-Si to TiO_2.*

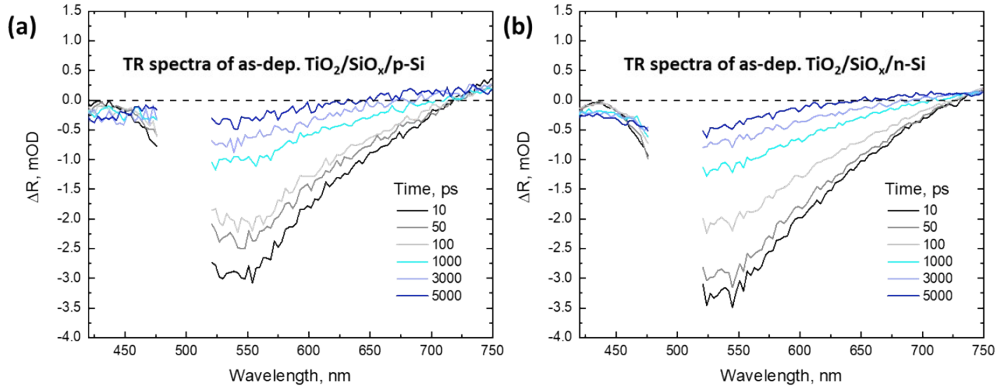

Figure S4*: Measured TR spectra of (a) as-dep. TiO_2/SiO_x/p-Si and (b) as-dep. TiO_2/SiO_x/n-Si samples with excitation at 500 nm.*

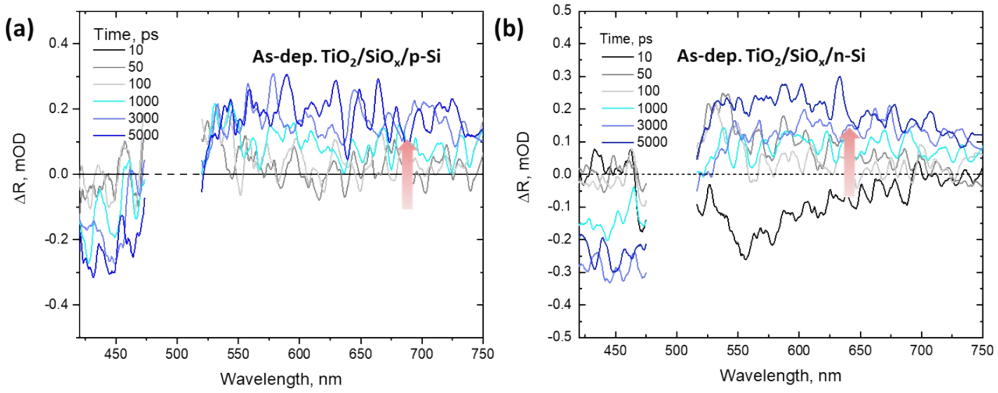

Figure S5: *Extracted CT spectra of (a) as-dep. TiO_2/SiO_x/p-Si and (b) as-dep. TiO_2/SiO_x/n-Si samples. The arrows indicate electrons moving from Si to TiO_2 with excitation at 500 nm.*

7. CT signal of samples after longer annealing durations

The HF-treated TiO_2/Si samples were annealed at 300 °C for longer durations to see the effect of heat treatment on CT and the passivation quality. The samples were excited at 500 nm and the charge carrier dynamics were compared at the 650 nm probe wavelength. The results

show that the prolonged thermal treatment at 300 °C for 60 and 90 minutes delays the CT process and extends the CT time because of the thermally introduced interfacial SiO_x layer even in the HF-treated Si samples. The results can be seen in Figure S6b where CT signal can only be observed at >1 ns timescale in the annealed samples as compared to the mere as-deposited samples where the CT rise could be observed within 200 ps. The carrier dynamics of the HF-treated as-dep. TiO_2/p-Si samples at different wavelengths are shown in Figure S6a.

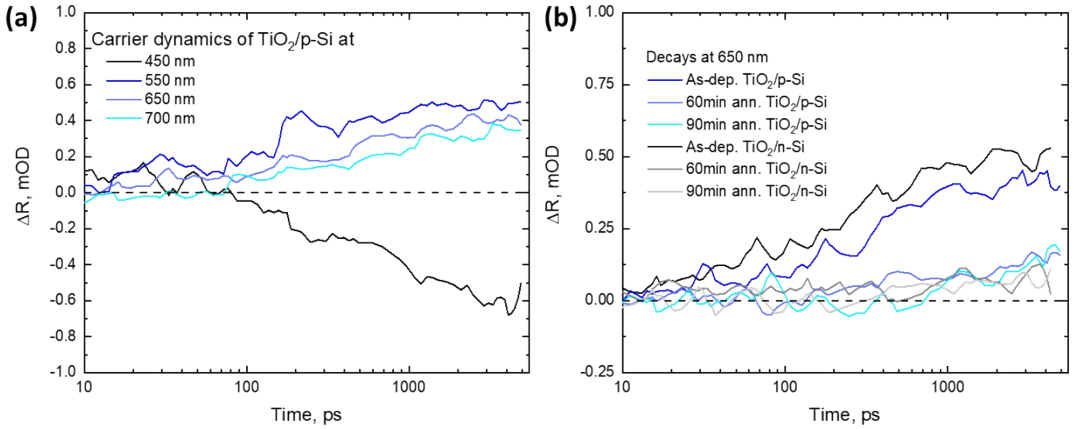

Figure S6: *Excitation of samples at 500 nm excitation to analyze (a) the rise of CT signal from Si to TiO_2 in as-dep. TiO_2/p-Si sample at different wavelengths and (b) comparison of the CT signal rise at the probe wavelength of 650 nm when the samples are annealed at 300 °C for 60 and 90 minutes.*

Table S3: *Excitation of samples at 500 nm excitation (200 μJ cm^{-2}) to analyze the characteristic charge transfer time in TiO_2/p-Si heterojunctions annealed at 250 °C for different durations.*

TiO_2/p-Si (HF-treated series)	**Characteristic CT time**	**TiO_2/SiO_x/p-Si (RCA2-treated series)**	**Characteristic CT time**
As-deposited	200 ps	As-deposited	3 ns
5min annealed	250 ps	5min annealed	>5 ns
10min annealed	400 ps	10min annealed	>5 ns
15min annealed	1 ns	15min annealed	>5 ns

When the samples are annealed at 300 °C for longer duration, the CT signal still can be observed at a characteristic CT time of >5 ns and no signal decay at the longer timescale is observed (Figure S6). However, in case of our previous study, when the samples were annealed at high temperatures, i.e., > 300 °C, the CT signal started to show decay at the longer timescales as shown in Figure S7.[8] This happened as the charge carriers at the TiO_2—Si interface started to recombine. However, this phenomenon is not yet observed in the current set of samples.

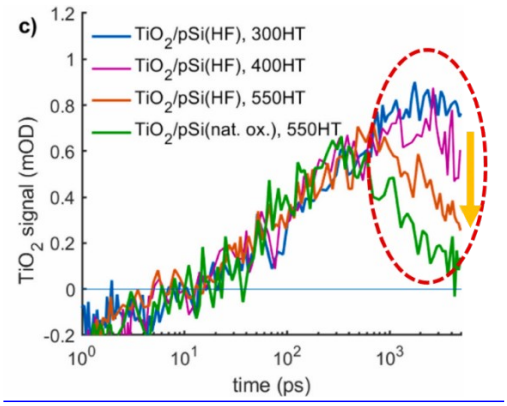

Figure S7: *Decay profiles after 500 nm excitation of different TiO_2/pSi samples probed at 700 nm, showing increased carrier losses in TiO_2 when the heat-treatment temperature is increased from 300 °C to 550 °C.[8] Reprinted with permission from ref 8. Copyright (2023) Elsevier BV.*

8. Surface properties and charge carrier dynamics of TiO_2

In order to study the effect of annealing on the carrier dynamics of TiO_2 solely, the TiO_2/Si samples were excited at 320 nm so that only TiO_2 films could be excited. The carrier dynamics of the as-dep. and annealed TiO_2 were compared at 600 nm probe wavelength. No big differences in the carrier lifetimes were observed when the samples were annealed at 250 °C up to 15 minutes. However, the lifetime slightly enhances when the samples were annealed at 300 °C (the onset temperature for crystallization) for 60 and 90 minutes as shown in **Figure S7**. Also, to monitor the changes in the morphology of TiO_2 thin films before and after the heat treatment, AFM images of the samples were taken. The results are presented in **Figure S8** and show that by the heat treatment, the samples undergo structural and compositional changes in them, which induces change in the surface roughness of the films.

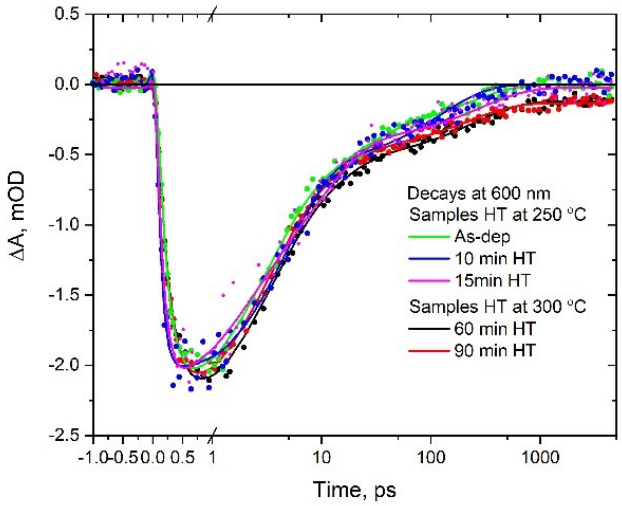

Figure S8: *Comparison of charge carrier dynamics of TiO_2/n-Si samples at 600 nm probe wavelength with excitation at 320 nm. HT is the abbreviation for heat-treatment (annealing).*

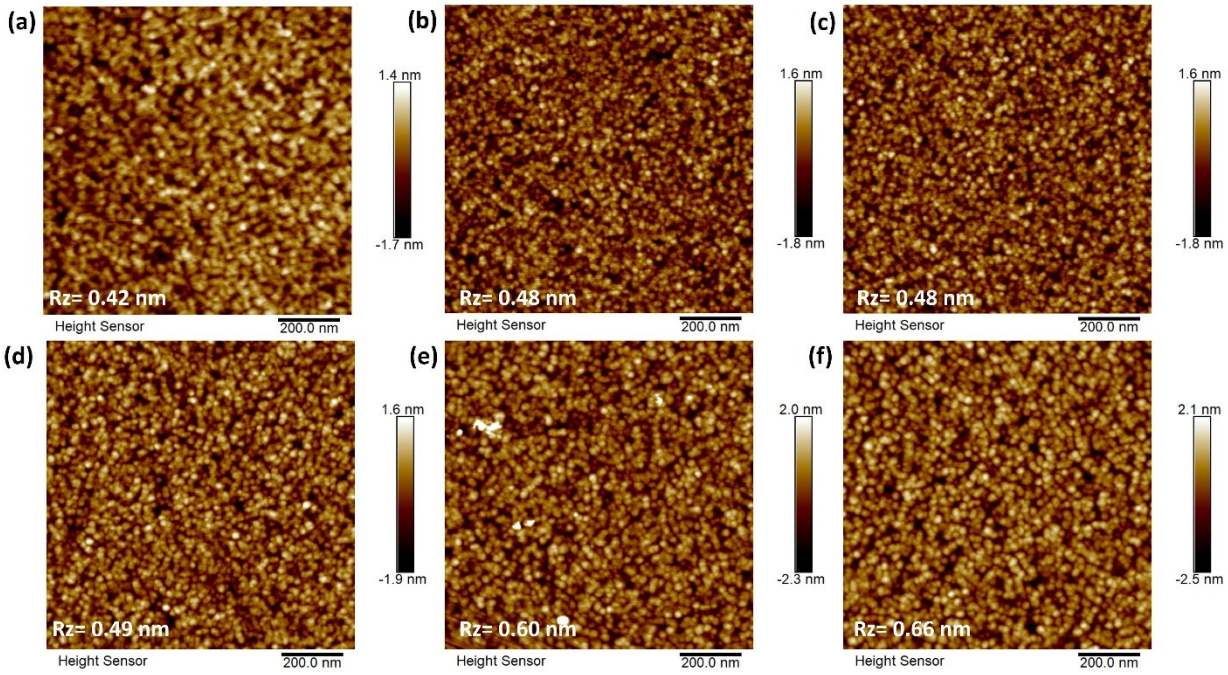

Figure S9: *1 µm × 1 µm AFM images of TiO_2/n-Si sample series annealed at 250°C for (a) as-dep. TiO_2/n-Si, (b) 5min TiO_2/n-Si, (c) 10min TiO_2/n-Si, (d) 15min TiO_2/n-Si, and TiO_2/n-Si sample series annealed at 300 °C for (e) 60min TiO_2/n-Si, and (f) 90min TiO_2/n-Si.*

9. Raman spectra of as-dep. and annealed samples

Regarding crystallinity, Raman spectra of the samples were measured after ALD and after 300 °C 90 min annealing. No change in spectra and no TiO_2 crystalline peaks (anatase or rutile) are found as shown in **Figure S9**.

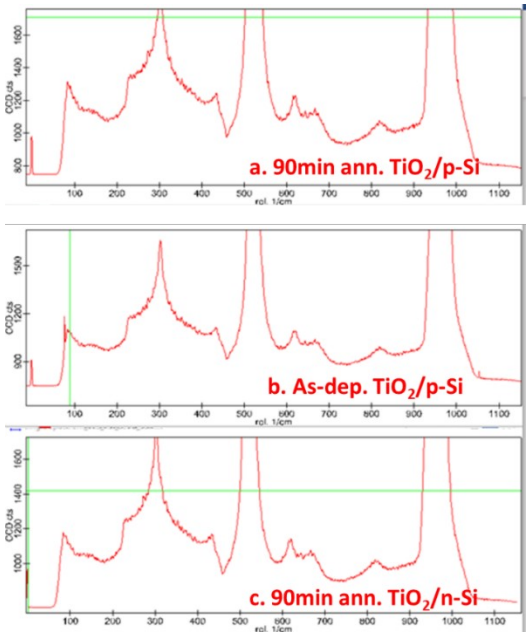

Figure S10: *Raman spectra of the as-deposited and annealed samples.*

References:

1. X. Yang, Q. Bi, H. Ali, K. Davis, W.V. Schoenfeld, K. Weber, Advanced Materials 28 (2016) 5891–5897.
2. K.M. Gad, D. Vössing, A. Richter, B. Rayner, L.M. Reindl, S.E. Mohney, M. Kasemann, IEEE Journal of Photovoltaics 6 (2016) 649–653.
3. T.-C. Chen, T.-C. Yang, H.-E. Cheng, I.-S. Yu, Z.-P. Yang, Applied Surface Science 451 (2018) 121–127.
4. Y. Nakagawa, K. Gotoh, M. Wilde, S. Ogura, Y. Kurokawa, K. Fukutani, N. Usami, Journal of Vacuum Science & Technology A 38 (2020) 022415.
5. K. Gotoh, T. Mochizuki, T. Hojo, Y. Shibayama, Y. Kurokawa, E. Akiyama, N. Usami, Current Applied Physics 21 (2021) 36–42.
6. K. Gotoh, H. Miura, A. Shimizu, Y. Kurokawa, N. Usami, Jpn. J. Appl. Phys. 60 (2021) SBBF04.
7. B. Liao, N. Dwivedi, Q. Wang, R.J. Yeo, A.G. Aberle, C.S. Bhatia, A. Danner, IEEE Journal of Photovoltaics 11 (2021) 319–328.
8. R. Khan, H.P. Pasanen, H. Ali-Löytty, H.M. Ayedh, J. Saari, V. Vähänissi, M. Valden, H. Savin, N.V. Tkachenko, Surfaces and Interfaces 38 (2023) 102871.